IEEE Access
Multidisciplinary | Rapid Review | Open Access Journal

Received June 5, 2019, accepted June 17, 2019, date of publication June 28, 2019, date of current version August 9, 2019.

Digital Object Identifier 10.1109/ACCESS.2019.2925570

Double-Loop Structure Integral Sliding Mode Control for UUV Trajectory Tracking

JUAN LI[1,2], HAO GUO[2], HONGHAN ZHANG[2], AND ZHEPING YAN[2]
[1]Science and Technology on Underwater Vehicle Technology, Harbin Engineering University, Harbin 150001, China
[2]College of Automation, Harbin Engineering University, Harbin 150001, China

Corresponding author: Honghan Zhang (zhanghonghan2008@163.com)

This work was supported in part by the National Natural Science Foundation of China under Grant 51609046/E091002, and in part by the Research Fund from Science and Technology on Underwater Vehicle Technology under Grant 614221502061701.

ABSTRACT To solve the problem of trajectory tracking control for the underactuated unmanned underwater vehicle (UUV) in external current disturbance, a back-stepping sliding mode control method with double-loop structure is proposed in this paper. The outer-loop controller constructs the position error sliding surface through desired position error, obtains the kinematics control law by combining with power reaching law, and gets the error of virtual velocity after completing the design of trajectory tracking kinematics controller. The inner-loop controller constructs the sliding surface of longitudinal, horizontal, and vertical velocity error, respectively, with the help of the UUV speed error. Also, the trajectory tracking dynamic controller is designed by combining with the exponential reaching law, where the control moment is almost chattering-free. The stability of the double-loop control system is proved by combining with the Lyapunov stability theory. Finally, the simulation experiments verify the high effectiveness of the algorithm.

INDEX TERMS UUV, trajectory tracking, integral sliding mode control, double-loop control structure.

I. INTRODUCTION

UUV has been used in deep-sea exploration, hydrological information collection, seabed topography and geomorphology exploration widely. The trajectory tracking control problem of UUV refers to correcting its position and velocity timely, and reaching the desired position in the specific time with specific attitude based on the position and velocity of desired trajectory. Due to a series of characteristics of UUV, including under-actuation, strong coupling, nonlinear and so on, and the influence of external disturbances such as waves and currents during operation, it is still a great challenge of researching on trajectory tracking control of UUV.

Backstepping control method [1]–[8] and sliding mode control method have been widely used [9]–[17] and [19]–[21]. Aiming at the problem of trajectory tracking backstepping control for underactuated UUV three-dimensional target, bio-inspired model and backstepping method are introduced to solve the problem of tracking shock caused by motion parameters jumping of the controller at turning points in reference [5]. Meanwhile, the singular value problem during single backstepping control is avoided. In addition, it analyses the stability of the whole closed-loop control system through the Lyapunov stability theory under the idea of backstepping design. In order to solve the problem of tracking the horizontal target trajectory for underactuated UUV with the conditions of parameter perturbation and constant current disturbance, the reference [10] applies the position error of the PID sliding mode stabilization control. The longitudinal velocity error and heading angular velocity error of first-order sliding surface and second-order sliding surface stabilization, and proves the limited global time convergence of the closed-loop system by use of Lyapunov stability theory and Cascade system theory. Reference [11] puts forward a control method of double-loop chattering-free adaptive sliding mode to solve the three-dimensional target trajectory tracking control of actuated UUV. It has the outer-loop position controller and inner-loop speed controller, and overcomes the outer-loop chattering by using saturation function instead of sign function. Moreover, a continuous adaptive term is designed to replace the discontinuous switching of traditional sliding mode, and global asymptotically stable of double-loop control system is proved by using Lyapunov stability theory. On the horizontal target trajectory tracking of underactuated UUV, the hyperbolic tangent is added to the original error equation. Three terminal sliding mode surfaces are designed based on longitudinal and transverse velocity error in reference [12]. It includes terminal sliding mode

The associate editor coordinating the review of this manuscript and approving it for publication was Salman Ahmed.

surface, fast terminal sliding mode surface and non-singular terminal sliding mode surface. Combining the constant speed approaching law with boundary layer function, a kind of horizontal trajectory tracking controller is designed and the finite time stability of the control system is analyzed. The simulation results are satisfactory. In reference [14], a sliding mode controller with adaptive gain is proposed for the horizontal target trajectory tracking sliding mode control of actuated UUV. It is a kind of sliding mode controller with adaptive gain. The reaching law replaces the original sign function reduces chattering with continuous item, and cooperates with adaptive law to estimate reaching law. In additional, it proves that the controller is finite time convergence. The simulation results show that the sliding mode gain of the controller is lower under the same conditions.

Aiming at the underactuated UUV with horizontal and vertical motion-missing actuator on the condition of current disturbance, this paper divides the control system into the kinematic controller subsystem and dynamic controller subsystem with the idea of backstepping control. The stabilization position error of virtual control input is gained through constructing Lyapunov function directly. The virtual control input is considered as expected value. The control law stabilization velocity error of force and torque is gained by designing integral sliding surface of velocity error. Compared with the single backstepping controller, the application of integral sliding mode control method with double-loop structure simplifies the design of controller. The application of integral sliding method for the inner loop can improves the dynamic performance of the system at the same time.

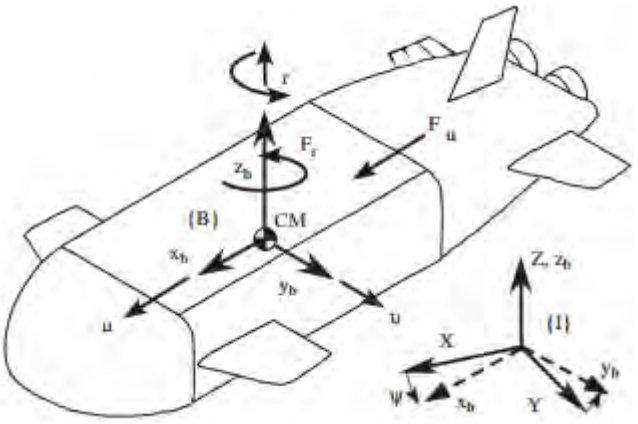

FIGURE 1. Structural diagram of underactuated UUV.

II. PROBLEM DESCRIPTION

As shown in Fig. 1, the UUV models are selected from references [2] and [18] as simulation objects. The UUV is equipped with three groups of independent actuators including fore-and-aft, heading and diving. It can realize the motion control with three degrees of freedom. It belongs to underactuated UUV, so the sway, roll and heave motion cannot be realized.

A. UUV MOTION MODEL

The six degrees of freedom kinematics equation of UUV is shown in Fig. 1.

$$\begin{cases} \dot{\xi} = u\cos\psi\cos\theta + v(\cos\psi\sin\theta\sin\varphi - \sin\psi\cos\varphi) \\ +w(\cos\psi\sin\theta\cos\varphi + \sin\psi\sin\varphi) \\ \dot{\eta} = u\sin\psi\cos\theta + v(\sin\psi\sin\theta\sin\varphi + \cos\psi\cos\varphi) \\ +w(\sin\psi\sin\theta\cos\varphi - \cos\psi\sin\varphi) \\ \dot{\zeta} = -u\sin\theta + v\cos\theta\sin\varphi + w\cos\theta\cos\varphi \\ \dot{\varphi} = p + q\sin\varphi\tan\theta + r\cos\varphi\tan\theta \\ \dot{\theta} = q\cos\varphi - r\sin\varphi \\ \dot{\psi} = q\sin\varphi/\cos\theta + r\cos\varphi/\cos\theta \end{cases} \tag{1}$$

where ξ, η, ζ *are* the position variables of UUV in the stability axis. $\dot{\xi}$, $\dot{\eta}$ and $\dot{\zeta}$ are the first-order time derivative of corresponding position variables, i.e. the linear velocity of UUV in the stability axis. ψ, θ, ϕ are the yaw angle, pitch angle and roll angle of UUV respectively, and $|\psi| < \pi$, $|\theta| < \pi/2$, $|\phi| < \pi/2$. u, v, w are the Linear velocity variables of UUV in the current axis.

In order to realize the trajectory tracking control of UUV, it is necessary to establish the dynamic model of UUV and the second-order dynamic equations of underactuated UUV, such as (2):

$$\begin{aligned} \frac{F_u}{m_{11}} &= \dot{u} - \frac{m_{22}}{m_{11}}vr + \frac{m_{33}}{m_{11}}wq + \frac{X_u}{m_{11}}u + \frac{X_{u|u|}}{m_{11}}u|u| \\ 0 &= \dot{v} + \frac{m_{11}}{m_{22}}ur + \frac{Y_v}{m_{22}}v + \frac{Y_{v|v|}}{m_{22}}v|v| \\ 0 &= \dot{w} - \frac{m_{11}}{m_{33}}uq + \frac{Z_w}{m_{33}}w + \frac{Z_{w|w|}}{m_{33}}w|w| \end{aligned}$$

then,

$$\begin{aligned} \frac{F_q}{m_{55}} &= \dot{q} - \frac{m_{33} - m_{11}}{m_{55}}uw + \frac{M_q}{m_{55}}q + \frac{M_{q|q|}}{m_{55}}q|q| \\ &\quad + \frac{\overline{BG}_z W\sin\theta}{m_{55}} \\ \frac{F_r}{m_{66}} &= \dot{r}_e - \frac{m_{11} - m_{22}}{m_{66}}uv + \frac{N_r}{m_{66}}r + \frac{N_{r|v|}}{m_{66}}r|r| \end{aligned} \tag{2}$$

where m_{ii} represents the hydrodynamic coefficient of UUV, F_u means the Longitudinal force of UUV, F_q means the pitching torque of UUV, and F_r represents the horizontal torque of UUV. It can be got that the UUV does not contain forces and torque in the dynamic equations of horizontal and vertical motion. So the UUV is underactuated.

B. ESTABLISHMENT OF SPACE TRAJECTORY TRACKING ERROR EQUATION

During space trajectory tracking, the motion of UUV has six degrees of freedom, including surge, sway, heave, pitch, roll and yaw. When implementing control strategy to UUV, the roll motion of UUV is usually neglected and only the other five degrees of freedom are considered. The error variables are shown as follows:

$$\begin{aligned} &\xi_e = \xi - \xi_p, \eta_e = \eta - \eta_p, \zeta_e = \zeta - \zeta_e \\ &\psi_e = \psi - \psi_p, \theta_e = \theta - \theta_p \end{aligned} \tag{3}$$

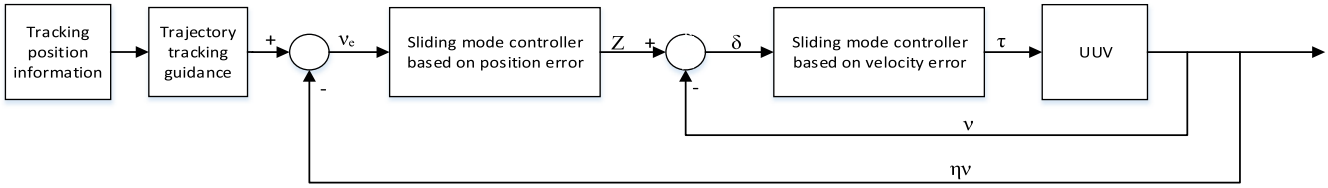

FIGURE 2. Block diagram of UUV trajectory tracking control system with double closed loop structure.

$$u_e = u - u_p, v_e = v - v_p, w_e = w - w_p$$
$$r_e = r - r_p, q_e = q - q_p \tag{4}$$

where ξ_p, η_p and ζ_p are the desired position amount of UUV in the stability axis respectively. ψ_p and θ_p are the expected values of yaw angle and pitch angle of UUV, and $\psi_p = \arctan(\dot{\eta}_p/\dot{\xi}_p)$, $\theta_p = -\arctan(\dot{\zeta}_p/\sqrt{\dot{\xi}_p^2 + \dot{\eta}_p^2})$. u_p and v_p are the expected linear velocity of UUV in the current axis, and $u_{p0} = \sqrt{\xi_p^2 + \eta_p^2 + \zeta_p^2}$, $v_{p0} = 0$, $w_{p0} = 0$. r_p is the yaw angle velocity, and q_p is the pitch angle velocity of UUV.

Plugging formulas (3) and (4) into formula (1), the kinematic error equations are obtained as follows:

$$\begin{bmatrix} \dot{\xi}_e \\ \dot{\eta}_e \\ \dot{\zeta}_e \end{bmatrix} = \begin{bmatrix} \cos\psi\cos\theta - \cos\psi_p\cos\theta_p & -\sin\psi + \sin\psi_p \\ \sin\psi\cos\theta - \sin\psi_p\cos\theta_p & \cos\psi - \cos\psi_p \\ -\sin\theta + \sin\theta_p & 0 \end{bmatrix} \begin{bmatrix} \cos\psi\sin\theta - \cos\psi_p\sin\theta_p \\ \sin\psi\sin\theta - \sin\psi_p\sin\theta_p \\ \cos\theta - \cos\theta_p \end{bmatrix} \begin{bmatrix} u_p \\ v_p \\ w_p \end{bmatrix} + \begin{bmatrix} \cos\psi\cos\theta & -\sin\psi & \cos\psi\sin\theta \\ \sin\psi\cos\theta & \cos\psi & \sin\psi\sin\theta \\ -\sin\theta & 0 & \cos\theta \end{bmatrix} \begin{bmatrix} u_e \\ v_e \\ w_e \end{bmatrix} \tag{5}$$

$$\dot{\theta}_e = q_e \tag{6}$$

$$\dot{\psi}_e = \frac{r}{\cos\theta} - \frac{r_p}{\cos\theta_p} \tag{7}$$

The corresponding dynamic error equation of underactuated UUV is as follows:

$$\dot{u}_e = \frac{m_{22}}{m_{11}}(v_e r_e + v_e r_p + v_p r_e + v_p r_p) - \frac{m_{33}}{m_{11}}(w_e q_e + w_e q_p + w_p q_e + w_p q_p) \frac{X_u}{m_{11}}(u_e + u_p) - \frac{X_{u|u|}}{m_{11}}(u_e + u_p)\left|u_e + u_p\right| - \dot{u}_p + \frac{F_u}{m_{11}} \tag{8}$$

$$\dot{v}_e = -\frac{m_{11}}{m_{22}}\left(u_e r_e + u_e r_p + u_p r_e + u_p r_p\right) - \frac{Y_v}{m_{22}}\left(v_e + v_p\right) - \frac{Y_{v|v|}}{m_{22}}\left(v_e + v_p\right)\left|v_e + v_p\right| - \dot{v}_p \tag{9}$$

$$\dot{w}_e = \frac{m_{11}}{m_{33}}\left(u_e q_e + u_e q_p + u_p q_e + u_p q_p\right) - \frac{Z_w}{m_{33}}\left(w_e + w_p\right) - \frac{Z_{w|w|}}{m_{33}}\left(w_e + w_p\right)\left|w_e + w_p\right| - \dot{w}_p \tag{10}$$

$$\dot{q}_e = \frac{m_{33} - m_{11}}{m_{55}}\left(u_e w_e + u_e w_p + u_p w_e + u_p w_p\right) - \frac{M_q}{m_{55}}\left(q_e + q_p\right) - \frac{M_{q|q|}}{m_{55}}\left(q_e + q_p\right)\left|q_e + q_p\right| - \frac{\overline{BG_z}W\sin\theta}{m_{55}} - \dot{q}_p + \frac{F_q}{m_{55}} \tag{11}$$

$$\dot{r}_e = \frac{m_{11} - m_{22}}{m_{66}}(u_e v_e + u_e v_p + u_p v_e + u_p v_p) - \frac{N_r}{m_{66}}\left(r_p + r_e\right) - \frac{N_{r|r|}}{m_{66}}(r_e + r_p)\left|r_e + r_p\right| - \dot{r}_p + \frac{F_r}{m_{66}} \tag{12}$$

Then the kinematic error equation and dynamic error equation of UUV space moving target trajectory tracking are established. Thus, the satisfied conditions of trajectory tracking can be described as:

$$\lim_{t\to\infty} |\xi_e| = 0, \quad \lim_{t\to\infty} |\eta_e| = 0, \quad \lim_{t\to\infty} |\zeta_e| = 0$$

when the above three conditions are satisfied, zero error trajectory tracking can be realized.

III. THE DESIGN OF UNDERACTUATED UUV SPACE TRAJECTORY TRACKING CONTROLLER

The block diagram of control system with double closed-loop structure is shown as Fig. 2. From it, It can be knew that the outer loop obtains the virtual velocity error variable through defining the position error sliding surface, and the inner loop tracks the virtual velocity error through defining the velocity error integral sliding surface. Finally, the trajectory tracking control of UUV is realized.

A. THE DESIGN OF OUTER LOOP CONTROLLER BASED ON POSITION ERROR SLIDING SURFACE

In order to realize the stabilization of the position error ξ_e, η_e and ζ_e of underactuated UUV, the following position error sliding surface is defined.

$$\begin{bmatrix} S_{01} \\ S_{02} \\ S_{03} \end{bmatrix} = \begin{bmatrix} \xi - \xi_p \\ \eta - \eta_p \\ \zeta - \zeta_p \end{bmatrix} \tag{13}$$

Find the first derivative of time t to formula (13) of position error sliding surface, and get:

$$\begin{bmatrix} \dot{S}_{01} \\ \dot{S}_{02} \\ \dot{S}_{03} \end{bmatrix} = \begin{bmatrix} \dot{\xi}_e \\ \dot{\eta}_e \\ \dot{\zeta}_e \end{bmatrix} \tag{14}$$

The kinematics error equation (5) is introduced into the first derivative (14) of the position error sliding surface

to obtain:

$$\begin{bmatrix} \dot{S}_{01} \\ \dot{S}_{02} \\ \dot{S}_{03} \end{bmatrix} = (R_1 - R_2) \begin{bmatrix} u_p \\ v_p \\ w_p \end{bmatrix} + R_1 \begin{bmatrix} u_e \\ v_e \\ w_e \end{bmatrix} \tag{15}$$

Among them,

$$R_1 = \begin{bmatrix} \cos\psi\cos\theta & -\sin\psi & \cos\psi\sin\theta \\ \sin\psi\cos\theta & \cos\psi & \sin\psi\sin\theta \\ -\sin\theta & 0 & \cos\theta \end{bmatrix},$$

$$R_2 = \begin{bmatrix} \cos\psi_p\cos\theta_p & -\sin\psi_p & \cos\psi_p\sin\theta_p \\ \sin\psi_p\cos\theta_p & \cos\psi_p & \sin\psi_p\sin\theta_p \\ -\sin\theta_p & 0 & \cos\theta_p \end{bmatrix}$$

In order to gain a better reaching effect, it can take the power approach law and have:

$$\begin{bmatrix} \dot{S}_{01} \\ \dot{S}_{02} \\ \dot{S}_{03} \end{bmatrix} = \begin{bmatrix} -\lambda_{01}\left|S_{01}\right|^{\alpha_{01}} sign\left(S_{01}\right) \\ -\lambda_{02}\left|S_{02}\right|^{\alpha_{02}} sign\left(S_{02}\right) \\ -\lambda_{03}\left|S_{03}\right|^{\alpha_{03}} sign\left(S_{03}\right) \end{bmatrix} \tag{16}$$

where $\lambda_{01} > 0$, $\lambda_{02} > 0$ and $\lambda_{03} > 0$ are the switching gain of sliding mode control. The exponential approach coefficient of sliding mode control includes $0 < \alpha_{01} < 1$, $0 < \alpha_{02} < 1$ and $0 < \alpha_{03} < 1$.

By substituting formula (15) into formula (16), the position error sliding mode control law of motion error equation can be obtained. In fact, the control law represents the expected value of the longitudinal velocity error as well as the lateral velocity error which are shown as z_u and z_v, and the expected value of the vertical velocity error which is z_w respectively. The form is as follows.

$$\begin{bmatrix} z_u \\ z_v \\ z_w \end{bmatrix} = -R_1^{-1}(R_1 - R_2) \begin{bmatrix} u_p \\ v_p \\ w_p \end{bmatrix} - R_1^{-1} \begin{bmatrix} \lambda_{01}\left|\xi_e\right|^{\alpha_{01}} sign\left(\xi_e\right) \\ \lambda_{02}\left|\eta_e\right|^{\alpha_{02}} sign\left(\eta_e\right) \\ \lambda_{03}\left|\zeta_e\right|^{\alpha_{03}} sign\left(\zeta_e\right) \end{bmatrix} \tag{17}$$

Take the first-order derivative of time t to equation (17) and get:

$$\begin{aligned} \begin{bmatrix} \dot{z}_u \\ \dot{z}_v \\ \dot{z}_w \end{bmatrix} = & -\dot{R}_1^{-1}(R_1 - R_2) \begin{bmatrix} u_p \\ v_p \\ w_p \end{bmatrix} \\ & - R_1^{-1}\left(\dot{R}_1 - \dot{R}_2\right) \begin{bmatrix} u_p \\ v_p \\ w_p \end{bmatrix} \\ & - R_1^{-1}(R_1 - R_2) \begin{bmatrix} \dot{u}_p \\ \dot{v}_p \\ \dot{w}_p \end{bmatrix} \\ & - \dot{R}_1^{-1} \begin{bmatrix} \lambda_{01}\left|\xi_e\right|^{\alpha_{01}} sign\left(\xi_e\right) \\ \lambda_{02}\left|\eta_e\right|^{\alpha_{02}} sign\left(\eta_e\right) \\ \lambda_{03}\left|\eta_e\right|^{\alpha_{03}} sign\left(\zeta_e\right) \end{bmatrix} \\ & - R_1^{-1} \begin{bmatrix} \lambda_{01}\alpha_{01}\left|\xi_e\right|^{\alpha_{01}-1} \\ \lambda_{02}\alpha_{02}\left|\eta_e\right|^{\alpha_{02}-1} \\ \lambda_{03}\alpha_{03}\left|\zeta_e\right|^{\alpha_{03}-1} \end{bmatrix} \end{aligned} \tag{18}$$

On the effect of the position error sliding mode control law (17), the motion error equation is changed into the following form:

$$\begin{bmatrix} \dot{\xi}_e \\ \dot{\eta}_e \\ \dot{\zeta}_e \end{bmatrix} = \begin{bmatrix} -\lambda_{01}\left|\xi_e\right|^{\alpha_{01}} sign\left(\xi_e\right) \\ -\lambda_{02}\left|\eta_e\right|^{\alpha_{02}} sign\left(\eta_e\right) \\ -\lambda_{03}\left|\zeta_e\right|^{\alpha_{03}} sign\left(\zeta_e\right) \end{bmatrix} \tag{19}$$

Although under the action of the position error control law (17), the subsystem (19) can be stabilized after introducing the formula (13) of the position error sliding mode surface. It should be knew that the control law obtained from formula (17) is not the real physical quantity of underactuated UUV. The controller needs to be further designed at the dynamic level to obtain the force and moment control law.

B. THE DESIGN OF INNER LOOP CONTROLLER BASED ON INTEGRAL SLIDING MODE SURFACE OF TRAJECTORY VELOCITY ERROR

The position error sliding mode control law z_u, z_v and z_w defined above represents the expected values of longitudinal velocity error, transverse velocity error and vertical velocity error respectively. So the following errors are defined as follows:

$$\delta_{\mathrm{u}} = u_e - z_u, \quad \delta_{\mathrm{v}} = v_e - z_v, \quad \delta_w = w_e - z_w \tag{20}$$

In the first step, the integral sliding mode surface of heave velocity error is designed as follows:

$$S_1 = \delta_u + \lambda_1 \int_0^t \delta_u dt \tag{21}$$

where $\lambda_1 > 0$ is the integral sliding mode gain.

After finding the first-order derivative of time t to (21) and substituting (18) and (8) into (21) leads to:

$$\begin{aligned} \dot{S}_1 = \lambda_1\delta_{\mathrm{u}} + \Bigg(& \frac{m_{22}}{m_{11}} vr - \frac{m_{33}}{m_{11}} wq - \frac{X_u}{m_{11}} u \\ & - \frac{X_{u|u|}}{m_{11}} u\left|u\right| - \dot{u}_p - \dot{z}_u + \frac{F_u}{m_{11}} \Bigg) \end{aligned} \tag{22}$$

Considering the influence of ocean current and parameter perturbation on underactuated UUV motion, the exponential approach law is selected to improve the dynamic quality of the system in the following form:

$$\dot{S}_1 = -k_1 \cdot sign\left(S_1\right) - \varepsilon_1 S_1 \tag{23}$$

where k_1 is the constant velocity approach coefficient) and $k_1 > 0$. ε_1 is the exponential approach coefficient and $\varepsilon_1 > 0$.

Thus, the longitudinal velocity control law can be obtained from formulas (22) and (24) which are as follows:

$$\begin{aligned} F_u = & -\left(\hat{m}_{22} vr - \hat{m}_{33} wq - \hat{X}_u u - \hat{X}_{u|u|} u\left|u\right|\right) \\ & + m_{11}\left(-\lambda_1\delta_{\mathrm{u}} + \dot{u}_p + \dot{z}_u - k_1 sign\left(S_1\right) - \varepsilon_1 S_1\right) \end{aligned} \tag{24}$$

"^"means the estimated values of system model parameters and satisfies the conditions: $\left|m_{ii} - \hat{m}_{ii}\right| \leq M_{ii}$, $\left|X_u - \hat{X}_u\right| \leq \bar{X}_u$, $\left|X_{u|u|} - \hat{X}_{u|u|}\right| \leq \bar{X}_{u|u|}$. Meanwhile, the following definition form (25) is the reference to the sliding

mode switching gain, and appropriate adjustments can be made in simulation.

$$k_1 = \eta_1 \left\{ M_{22} |vr| + M_{33} |wq| + \bar{X}_u |u| + \bar{X}_{u|u|} u^2 + \left|\dot{u}_p\right| + M_{11} |\dot{z}_u| \right\}, \quad 0 < \eta_1 < 1 \tag{25}$$

The second step is to design the sliding surface of lateral velocity error integral. In lateral motion, the under-actuated UUV lacks executive structure, and stabilization of error δ_v is achieved by controlling vertical rudder. So the integral sliding surface is designed as:

$$S_2 = \dot{\delta}_v + \int_0^t \lambda_{21} \dot{\delta}_v + \lambda_{22} \delta_v dt \tag{26}$$

where $\lambda_{21} > 0$ and $\lambda_{22} > 0$ are the integral sliding mode gain.

Taking the first-order derivative of time t to equation (26) and substituting formula (18) leads to:

$$\dot{S}_2 = (\ddot{v}_e - \ddot{z}_v) + \lambda_{21} \dot{\delta}_v + \lambda_{22} \delta_v \tag{27}$$

Choosing the exponential reaching law to improve the dynamic quality, the form is as follows:

$$\dot{S}_2 = -k_2 \cdot sign\,(S_2) - \varepsilon_2 S_2 \tag{28}$$

where k_2 is the constant velocity approach coefficient and $k_2 > 0$. ε_2 is the exponential approach coefficient and $\varepsilon_2 > 0$.

The yaw angular velocity control laws can be obtained from formula (27), (28) and (12). The error δ_v can be stabilized by controlling the vertical rudder. When designing the yaw control laws, the expression form of F_r is as follows which contains term $\dot{r}$.

$$\begin{aligned} F_r = {} & \left(\hat{m}_{22} - \hat{m}_{11}\right) uv + \hat{N}_r r + \hat{N}_{r|r|} r\,|r| \\ & - \frac{\hat{m}_{66}}{\hat{m}_{22} z_u - \hat{m}_{22} z_v \tan\theta - \hat{m}_{11} u} \left(\hat{m}_{11} \dot{u} r + \hat{Y}_v \dot{v} \right. \\ & + 2\hat{Y}_{v|v|} sign\,(v)\, v\dot{v} - \hat{m}_{22} \left(\lambda_{21} \dot{\delta}_v + \lambda_{22} \delta_v + f\,(\cdot) - \ddot{v}_R \right) \\ & \left. - k_2 sign\,(S_2) - \varepsilon_2 S_2 \right) \end{aligned} \tag{29}$$

Among them, $\ddot{z}_v = -(z_v \tan\theta + z_u)\,\dot{r} + f\,(\cdot)$. Where k_2 is the constant velocity approach coefficient. Appropriate adjustments can be made during simulating by referring to the definition form of formula (30).

$$\begin{aligned} k_2 = {} & \eta_2 \left\{ (M_{66} + M_{11}) |uv| + \bar{N}_r |r| + \bar{N}_{r|r|} r^2 \right. \\ & + \frac{M_{22} M_{66}}{(M_{22} |z_u| + M_{22} |z_v \tan\theta| + M_{11} |u|)} |Y_v \dot{v} \\ & \left. + m_{11} \dot{u} r + 2 sign\,(v)\, Y_{v|v|} v\dot{v} + m_{22} \left(\ddot{v}_R + f\,(\cdot)\right) \right\}, \\ & 0 < \eta_2 < 1 \end{aligned} \tag{30}$$

The third step is to design the sliding surface of vertical velocity error integral. During vertical motion, because there is no actuator of underactuated UUV, so the calm of error δ_w is achieved by controlling the vertical rudder. The vertical velocity error integral sliding surface is defined as:

$$S_3 = \dot{\delta}_w + \int_0^t \lambda_{31} \dot{\delta}_w + \lambda_{32} \delta_w dt \tag{31}$$

Among it, $\lambda_{31} > 0$ and $\lambda_{32} > 0$ are the integral sliding mode gain.

Take the first-order derivative of time t to equation (31) leads to:

$$\dot{S}_3 = \ddot{\delta}_w + \lambda_{31} \dot{\delta}_w + \lambda_{32} \delta_w \tag{32}$$

Improve the dynamic quality of system through choosing constant speed approaching law. The form is as follows:

$$\dot{S}_3 = -k_3 \cdot sign\,(S_3) - \varepsilon_3 S_3 \tag{33}$$

where k_3 is the constant velocity approach coefficient, and $k_3 > 0$. ε_3 is the exponential approach coefficient, and $\varepsilon_3 > 0$.

The control law of pitch angular velocity can be obtained from formula (32), (33) and (11). The error δ_v can be stabilized by controlling the horizontal rudder. In order to gain the expression form of F_q which is as follows. The design of the pitch angular velocity control laws should contain term $\dot{q}$.

$$\begin{aligned} F_q = {} & -(m_{33} - m_{11})\, uw + M_{q|q|} q\,|q| \\ & + M_q q + \dot{q}_p + \overline{BG_z} W \sin\theta \\ & + \frac{1}{m_{33} w_p - m_{33} z_w + m_{11} u} \\ & \times (m_{11} m_{55} \dot{u} q - 2 m_{55} Z_{w|w|} w\dot{w} \cdot sign\,(w) \\ & + m_{33} m_{55} \left(f(\cdot) - \ddot{w}_p + \lambda_{31} \dot{\delta}_w + \lambda_{32} \delta_w \right) \\ & - m_{55} Z_w \dot{w} - k_3 sign\,(S_3) - \varepsilon_3 S_3) \end{aligned} \tag{34}$$

In the formula, $\ddot{z}_w = \left(z_w - u_p\right) \dot{q} + f\,(\cdot)$.

C. PROOF OF CONTROL SYSTEM STABILITY

1) OUTER-LOOP CONTROL SYSTEM

The stability of the longitudinal outer-loop control system is evaluated by choosing the following Lyapunov function as:

$$V_0 = \frac{1}{2} S_{01}^2 + \frac{1}{2} S_{02}^2 + \frac{1}{2} S_{03}^2 \tag{35}$$

Take the first-order derivative of time t to equation (35) leads to:

$$\begin{aligned} \dot{V}_0 &= \dot{S}_{01} S_{01} + \dot{S}_{02} \dot{S}_{02} + \dot{S}_{03} S_{03} \\ &= -\lambda_{01} |S_{01}|^{\alpha_{01}} sign\,(S_{01})\, S_{01} - \lambda_{02} |S_{02}|^{\alpha_{02}} \\ &\quad \times sign\,(S_{02})\, S_{02} - \lambda_{03} |S_{03}|^{\alpha_{03}} sign\,(S_{03})\, S_{03} \\ &= -\sum_{i=1}^{3} k_{0i} |S_{0i}|^{\alpha_{0i}+1} \\ &\le 0 \end{aligned} \tag{36}$$

The function is positive definite and the Lyapunov derivative (36) is negative definite by the definition (35). So the subsystem can be asymptotically stable under the action of outer-loop control law.

2) INNER-LOOP CONTROL SYSTEM

The stability of the longitudinal velocity inner-loop control system is evaluated by choosing the following Lyapunov function as

$$V_1 = \frac{1}{2}S_1^2 \tag{37}$$

Taking the first-order derivative of time t to equation (37) and substituting (22)-(24) into the above equation yields:

$$\begin{aligned}
\dot{V}_1 &= S_1\dot{S}_1 \\
&= S_1\left\{\lambda_1\delta_u + \frac{m_{22}}{m_{11}}vr - \frac{m_{33}}{m_{11}}wq - \frac{X_u}{m_{11}}u\right. \\
&\quad \left. -\frac{X_{u|u|}}{m_{11}}u|u| - \dot{u}_p + \frac{F_u}{m_{11}} - \dot{z}_u\right\} \\
&= S_1\left\{\lambda_1\delta_u + \frac{m_{22}}{m_{11}}vr - \frac{m_{33}}{m_{11}}wq - \frac{X_u}{m_{11}}u\right. \\
&\quad -\frac{X_{u|u|}}{m_{11}}u|u| - \dot{u}_p - \dot{z}_u + \frac{1}{m_{11}} \\
&\quad \times \left(-m_{22}vr + m_{33}wq + X_u u + X_{u|u|}u|u| - m_{11}\right. \\
&\quad \left.\left. \times \left(\dot{u}_p + z_u + \varepsilon_1 S_1 + k_1 \cdot sign\left(S_1\right) + \lambda_1\delta_u\right)\right)\right\} \\
&= -k_1\left|S_1\right| - \varepsilon_1 S_1^2
\end{aligned} \tag{38}$$

The function is positive definite and the Lyapunov derivative (36) is negative definite by the definition (37). So the subsystem can be asymptotically stable under the action of longitudinal velocity control law.

The stability of the yaw angular velocity control system is evaluated by choosing the following Lyapunov function as

$$V_2 = \frac{1}{2}S_2^2 \tag{39}$$

Taking the first-order derivative of time t to equation (37) and substituting (27)-(29) into the above equation yields:

$$\begin{aligned}
\dot{V}_2 &= S_2\dot{S}_2 \\
&= S_2\left\{\lambda_{21}\dot{\delta}_v + \lambda_{22}\delta_v + \left(-\frac{m_{11}}{m_{22}}(\dot{u}r + u\dot{r}) - \frac{Y_v}{m_{22}}\dot{v}\right.\right. \\
&\quad \left.\left. -2\cdot\frac{Y_{v|\dot{v}|}}{m_{22}}v\dot{v}\cdot sign(v) - \ddot{v}_R - \dddot{z}_v\right)\right\} \\
&= S_2\left\{\left(z_v\tan\theta + z_u - \frac{m_{11}}{m_{22}}u\right)\left(\frac{m_{11}-m_{22}}{m_{66}}uv\right.\right. \\
&\quad -\frac{N_r}{m_{66}}r - \frac{N_{rirr}}{m_{66}}r|r| - \dot{r}_R + \frac{F_r}{m_{66}}\Bigg) - \frac{Y_v}{m_{22}}\dot{v} \\
&\quad \left.\left. -2\cdot\frac{Y_{v\dot{v}\|}}{m_{22}}v\dot{v}\cdot sign(v) - \ddot{v}_R + f(\cdot) - \frac{m_{11}}{m_{22}}\dot{u}r\right\}\right. \\
&= -k_2\left|S_2\right| - \varepsilon_2 S_2^2
\end{aligned} \tag{40}$$

The function is positive definite and the Lyapunov derivative (36) is negative definite by the definition (39). So the subsystem can be asymptotically stable under the action of control law.

The stability of the pitch angular velocity control system is evaluated by choosing the following Lyapunov function as:

$$V_3 = \frac{1}{2}S_3^2 \tag{41}$$

Taking the first-order derivative of time t to equation (37) and substituting (32)-(34) into the above equation yields:

$$\begin{aligned}
\dot{V}_3 &= \dot{S}_3\dot{S}_3 \\
&= S_3\left\{\lambda_{31}\dot{\delta}_w + \lambda_{32}\delta_w + \left(\frac{m_{11}}{m_{33}}(\dot{u}q + u\dot{q}) - \frac{Z_w}{m_{33}}\dot{w}\right.\right. \\
&\quad \left.\left. -2\cdot\frac{Z_{w|\dot{w}\|}}{m_{33}}ww\cdot sign(w) - \ddot{w}_p - \dddot{z}_w\right)\right\} \\
&= S_3\left\{\left(u_p - z_w + \frac{m_{11}}{m_{33}}u\right)\left(\frac{m_{33}-m_{11}}{m_{55}}uw - \frac{M_q}{m_{55}}q\right.\right. \\
&\quad -\frac{M_{q|q|}}{m_{55}}q|q| - \frac{\overline{BG_z}W\sin\theta}{m_{55}} + \frac{F_q}{m_{55}}\Bigg) - \frac{Zw}{m_{33}}\dot{w} \\
&\quad \left.\left. -2\cdot\frac{Z_{w|w|}}{m_{33}}ww\cdot\mathrm{sign}(w) - \ddot{w}_p - f(\cdot) + \frac{m_{11}}{m_{33}}\dot{u}q\right\}\right. \\
&= -k_3\left|S_3\right| - \varepsilon_3 S_3^2
\end{aligned} \tag{42}$$

The function is positive definite and the Lyapunov derivative (36) is negative definite by the definition (41). So the subsystem can be asymptotically stable under the action of control law.

Analyzing the stability of closed-loop control system and choosing the following Lyapunov function as:

$$V = \frac{1}{2}S_{01}^2 + \frac{1}{2}S_{02}^2 + \frac{1}{2}S_{03}^2 + \frac{1}{2}S_1^2 + \frac{1}{2}S_2^2 + \frac{1}{2}S_3^2 \tag{43}$$

Take the first-order derivative of time t to equation (43) and get:

$$\begin{aligned}
\dot{V} &= S_{01}\dot{S}_{01} + S_{02}\dot{S}_{02} + S_{03}\dot{S}_{03} + S_1\dot{S}_1 + S_2\dot{S}_2 + S_3\dot{S}_3 \\
&= -\lambda_{01}\left|S_{01}\right|^{\alpha_{01}+1} - \lambda_{02}\left|S_{02}\right|^{\alpha_{02}+1} - \lambda_{03}\left|S_{03}\right|^{\alpha_{03}+1} \\
&\quad -k_1\left|S_1\right| - \varepsilon_1 S_1^2 - k_2\left|S_2\right| - \varepsilon_2 S_2^2 - k_3\left|S_3\right| - \varepsilon_3 S_3^2 \\
&= -\sum_{i=1}^{3}\left(k_{0i}\left|S_{0i}\right|^{\alpha_{0i}+1} + k_i\left|S_i\right| + \varepsilon_i S_i^2\right) \\
&\le 0
\end{aligned} \tag{44}$$

The function is positive definite and the Lyapunov derivative is negative definite by the definition (43)-(44). So the double-loop control system can be asymptotically stable under the action of control input (24), (29) and (34).

IV. THE SIMULATION EXPERIMENT ANALYSIS OF UUV TARGET SPACE MOVING TARGET TRAJECTORY TRACKING

The UUV of simulation experiment in this paper is selected from the simulation experiment objects of references [2] and [14]. The model parameters are as follows.

A. HORIZONTAL TRAJECTORY TRACKING SIMULATION EXPERIMENT

In this experiment, the horizontal moving target trajectory tracking controller method based on backstepping integral sliding mode is compared with the backstepping method. The design method of backstepping controller is shown in reference [2]. The reference trajectory of simulation experiments is defined as equation (37). The unit is m and time

TABLE 1. Model parameters.

Weight (kg)		m_{11}=215	m_{22}=265	m_{33}=265
The moment of inertia (kg*m2)		m_{44}=40	m_{55}=80	m_{66}=80
Linear damping parameter	kg/s	X_u=70	Y_v=100	Z_w=100
	m2/s	K_p=30	M_q=50	N_r=50
Secondary damping parameter	kg/m	$X_{u\|u\|}$=100	$Y_{v\|v\|}$=100	$Z_{w\|w\|}$=100
	Kg*m^2	$K_{p\|p\|}$=50	$M_{q\|q\|}$=100	$N_{r\|r\|}$=100
Metacenter (m)			$\overline{BG}_z$=0.2	

unit is s.

$$\begin{aligned} x_p &= 10\sin(0.01t) \quad 0 < t \le 700 \\ y_p &= 8\cos(0.01t) \quad 0 < t \le 700 \end{aligned} \tag{45}$$

The initial motion states of UUV are u = 0.01m/s, v = 0m/s and r = 0rad/s. The initial position and yaw angle are x = −1m, y = 11m, and φ = 0rad.The initial expected velocity of guidance method is up = 0.3m/s. The total time of simulation experiment is 700s and the iteration step is 0.01. The parameter settings, including reference trajectory and initial motion state of UUV, are consistent with those in reference [15].

Fig. 3 shows the tracking effect of UUV "elliptical" motion trajectory. The red solid line in the figure is the UUV motion trajectory with the backstepping integral sliding mode controller. The green dotted line is the UUV motion trajectory with the backstepping controller. The blue dotted line is the desired target trajectory. From the figure, it can be found that both methods can achieve elliptic trajectory tracking. From the right enlarged image, the performance of two methods is different. Fig. 4 is the UUV tracking position and the response curve of position error during trajectory tracking. It can be found that the initial errors are $|x_{e0}| = 1$, $|y_{e0}| = 3$, and the final error is 0. At the initial stage, the rising time of the backstepping controller is less than that of the backstepping integral sliding mode controller. The response speed is slightly faster, but the adjustment time is long. Fig. 5 means the tracking yawing, yaw angular velocity and the error response curves. In the yawing control, the response speed of the backstepping integral sliding mode controller is faster and the adjustment time is shorter. Fig. 6 shows the tracking speed and the speed error response. The response of the backstepping sliding mode control tracking curve is faster and the adjustment time is shorter, but the overshoots is larger. There are slight fluctuations of speed error near zero, and the steady-state errors of both methods are less than 0.01. Fig. 7 refers to the control input force and moment response curve. The sliding mode control curve has no chattering. Comprehensively, the speed error stabilization response speed of UUV is faster and the adjustment time is shorter by using the control

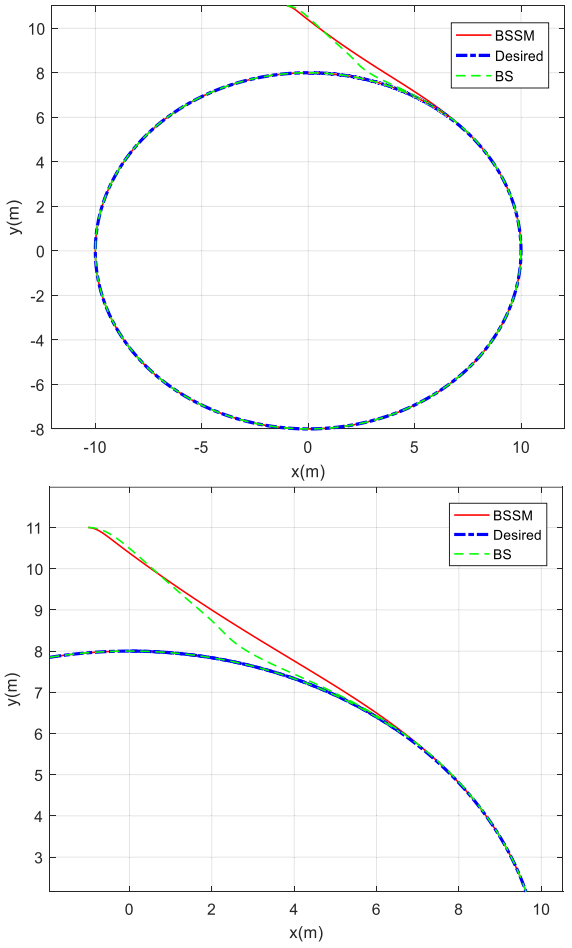

FIGURE 3. UUV trajectory.

method of backstepping integral sliding mode. While the position error response speed of UUV using backstepping control method is slightly faster, but the adjustment time has no advantage over the backstepping integral sliding mode. Compared with the single backstepping method, the design of the backstepping integral sliding mode control method is simpler.

B. SIMULATION EXPERIMENT OF SPACE TRAJECTORY TRACKING

1) SIMULATION EXPERIMENT 1: POLYLINE SHAPE SPATIAL TRAJECTORY TRACKING UNDER OCEAN CURRENT DISTURBANCE

Spatial trajectory setting is as follow:

$$x_p = \begin{cases} t & 0 < t < 300 \\ 1.3t90 & t \ge 300 \end{cases}$$

$$y_p = \begin{cases} 0.5t & 0 < t < 300 \\ 150 & 300 \le t < 500 \\ 0.5t - 100 & t \ge 500 \end{cases}$$

$$z_p = \begin{cases} 0.1t + 1 & 0 < t < 300 \\ 31 & 300 \le t < 500 \\ 0.1t - 19 & t \ge 500 \end{cases} \tag{46}$$

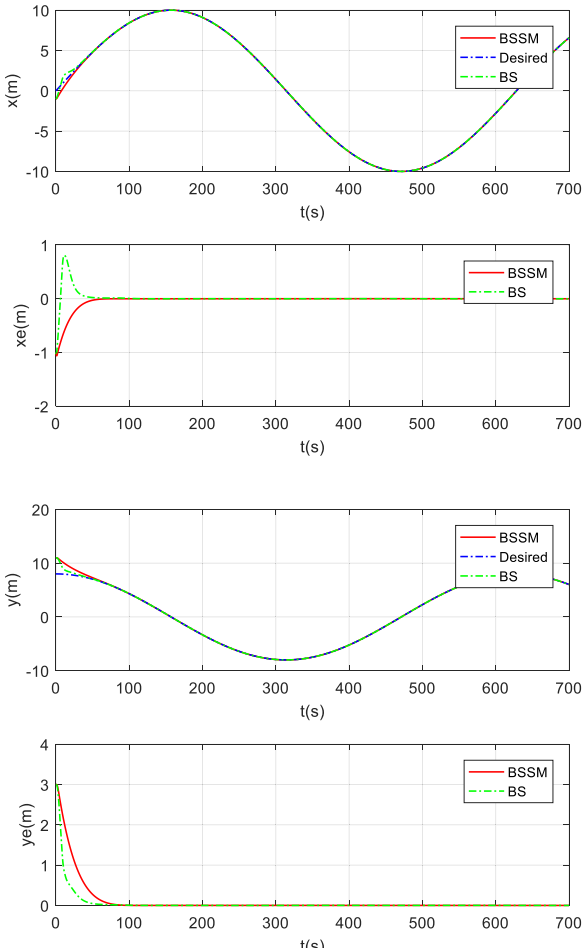

FIGURE 4. Tracking position and position error.

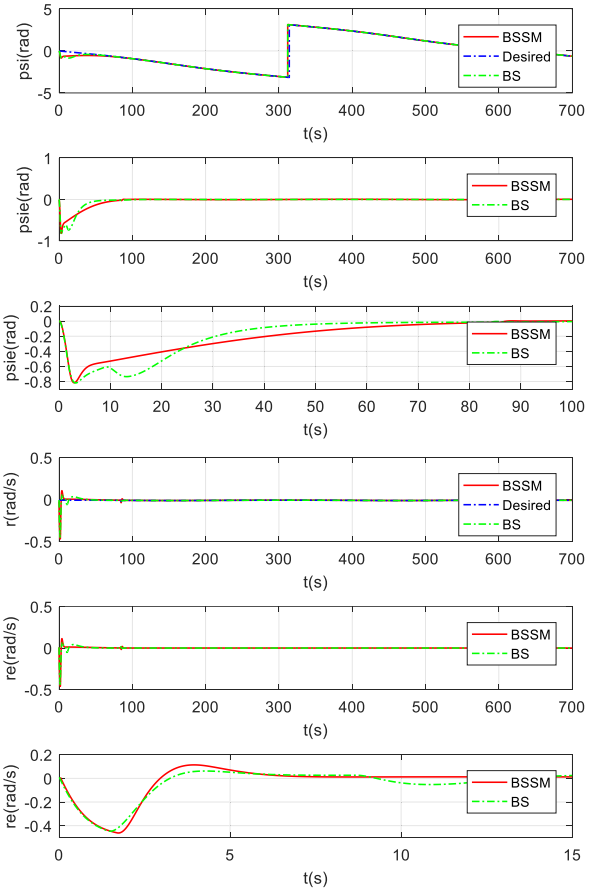

FIGURE 5. Yaw angle, yaw angular velocity and error.

The initial motion states of UUV are u_0 =0.01 m/s, v_0 = 0m/s, $w_0 = 0$ m/s, $q_0 = 0$ rad/s and $r_0 = 0$ rad/s. The initial position and yaw angle are $x_0 = -5$m, $y_0 = 15$ m, $z_0 = 5$m, $\theta_0 = 0$ rad and $\psi_0 = 0$rad respectively. The total duration of the simulation experiment is 700s and Sampling step size is 0.04.Considering constant current disturbance, the magnitude of current is 0.06m/s, and the flow direction is 45°.

Fig. 8 is the process chart of UUV tracking ''polyline shape'' space trajectory. The blue dotted line is the desired trajectory, and the red solid line is the actual trajectory of UUV. From the figure, it can be seen that UUV realizes the tracking of space linear trajectory.

Fig. 9 and Fig. 10 are projection trajectories of the trajectory on the xoy plane and the xoz plane respectively. In the initial stage, the position of UUV is quite different from the position of the desired trajectory, and gradually traces the upper polyline.

Fig. 11 and Fig. 12 means UUV yaw angle, pitch angle and their error curves respectively. During the period of 0-300 s, UUV yaw angle maintains 60 degrees after stabilization, and keeps linear yaw moving in the horizontal plane. During the period of 300-500 s, the yaw angle of UUV maintains 0 degrees after stabilization, and the UUV maintains direct route motion in the horizontal plane. During the period of 500-700 s, the yaw angle of UUV maintains 60 degrees after stabilization, and it keeps straight yaw motion in the horizontal plane. Within 0-300 seconds, the pitch angle remains around, and the UUV dives uniformly. The pitch angle of 300-500 s is kept around, and the UUV is kept in constant depth. UUV continued to dive at a uniform speed while the pitch angle remained near 500-700 s.

Fig. 13 shows the error response curves of the yaw angular velocity and the yaw angular velocity of UUV.

Fig. 14 shows the response curves of pitch angular velocity and pitch angular velocity error of UUV. It can be seen that the response speed of yaw angular velocity and pitch angular velocity is fast and the stable precision is good, but the overshoot of track connection time period is large. Fig. 15 is the variation curve of UUV position error. It can be seen that the position error of UUV is very small and only fluctuates slightly in a certain period of time. But the longitudinal position fluctuates least.

Fig. 16 and FIG. 17 are UUV control force, moment input curves and local enlargement maps. It can be seen that there is almost no chattering in control force and moment, and the force and moment change sharply at the initial stage of tracking and at the joint of trajectory. The reason is that there are large position and velocity differences between UUV and

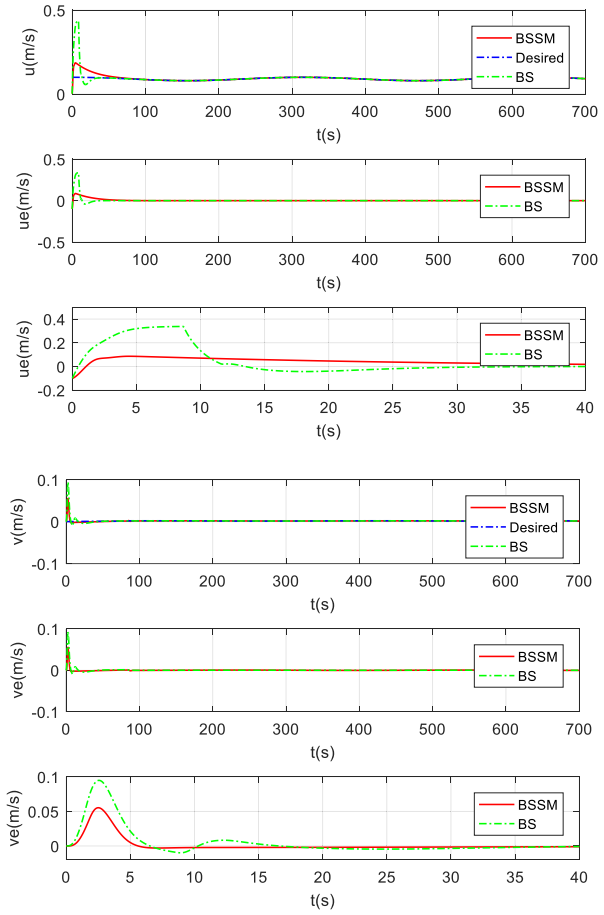

FIGURE 6. Velocity and velocity error.

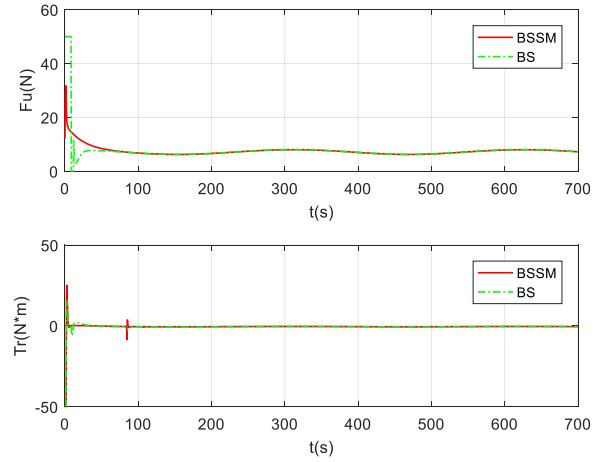

FIGURE 7. Force and torque input.

the target at the initial stage, and the large control input for fast and small errors.

2) SIMULATION EXPERIMENT 2: CURVE SPATIAL TRAJECTORY TRACKING UNDER EXTERNAL CURRENT DISTURBANCES

The space trajectory of the experiment is as follows:

$$x_p = \mathrm{t}$$

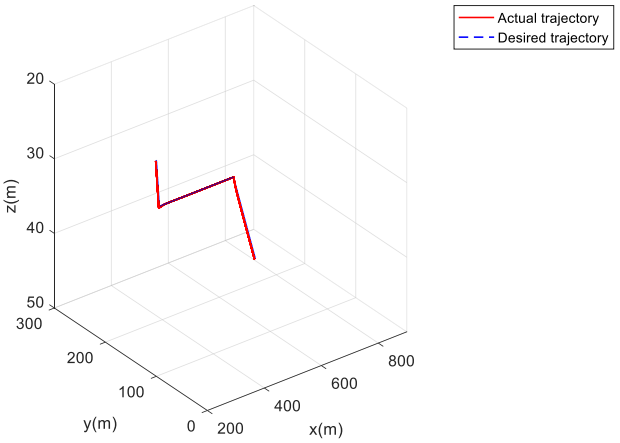

FIGURE 8. UUV trajectory.

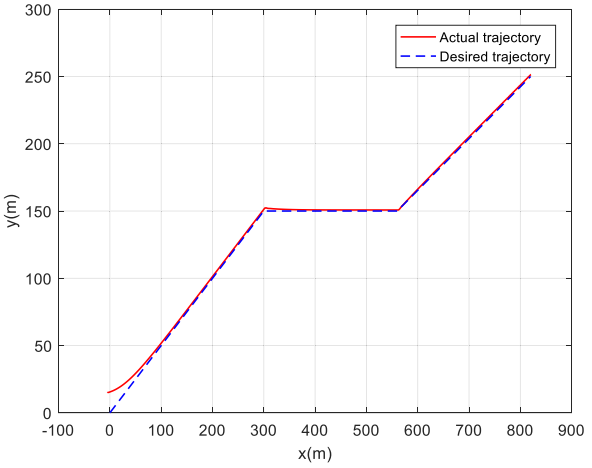

FIGURE 9. Motion trajectory projection on xoy axis.

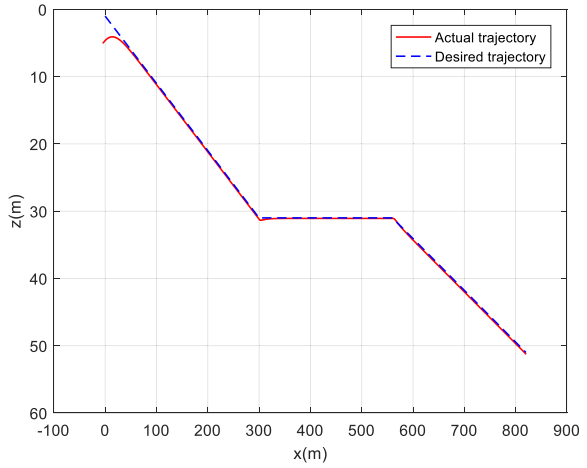

FIGURE 10. Motion trajectory projection on xoz axis.

$$\begin{aligned} y_p &= 25\sin(0.01t) \\ z_p &= 25\cos(0.02t) + 30 \end{aligned} \tag{47}$$

The initial motion states of UUV are $u_0 = 0.01$ m/s, $v_0 = 0$m/s, $w_0 = 0$ m/s, $q_0 = 0$ rad/s and $r_0 = 0$ rad/s. The initial position and yaw angle are $x_0 = 0$m, $y_0 = 0$ m, $z_0 = 40$ m,

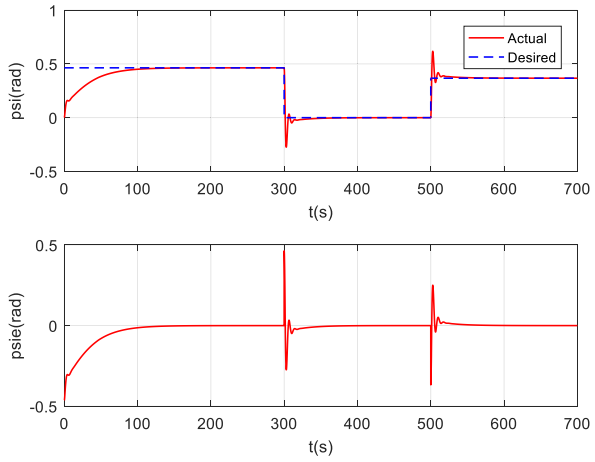

FIGURE 11. Yaw angle and angle error.

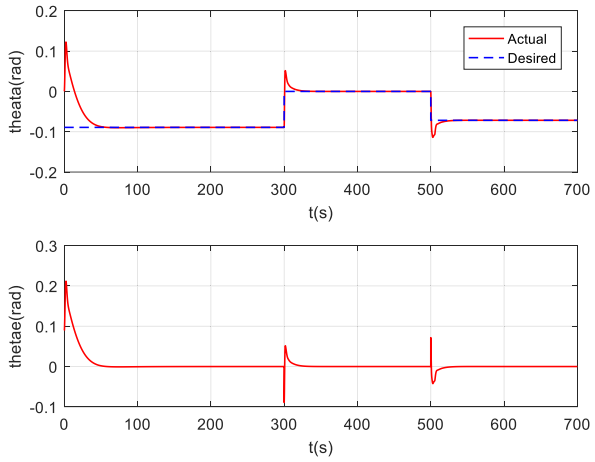

FIGURE 12. Pitch angle and angle error.

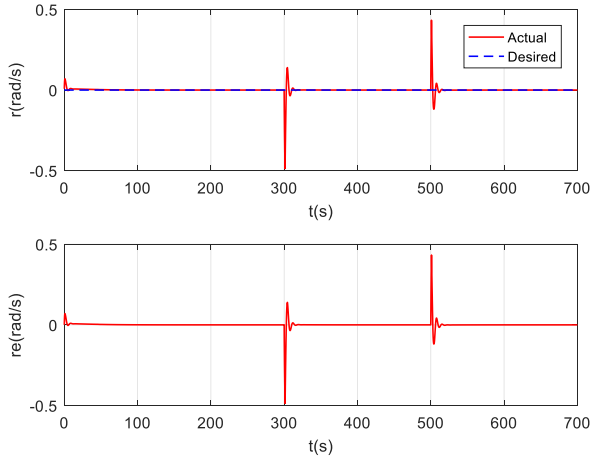

FIGURE 13. Yaw angular velocity and velocity error.

$\theta_0 = 0$ rad and $\psi_0 = 0$ rad respectively. The total duration of this simulation experiment is 900 s, and sampling step length is 0.04. The external current disturbances with current velocity 0.06 m/s and flow direction 45° are added.

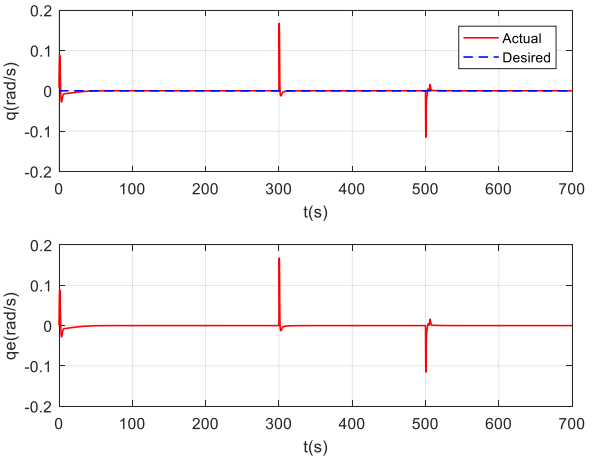

FIGURE 14. UUV position error.

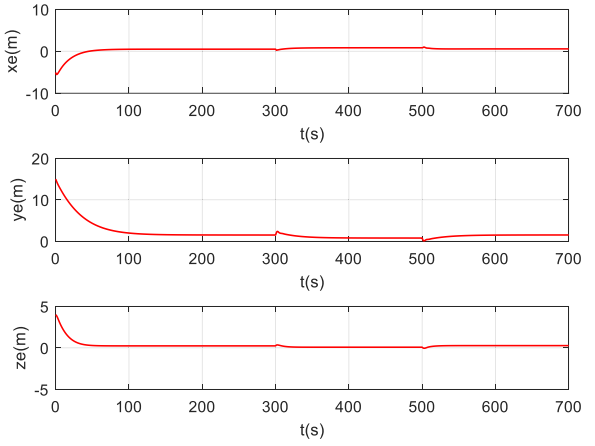

FIGURE 15. UUV position error.

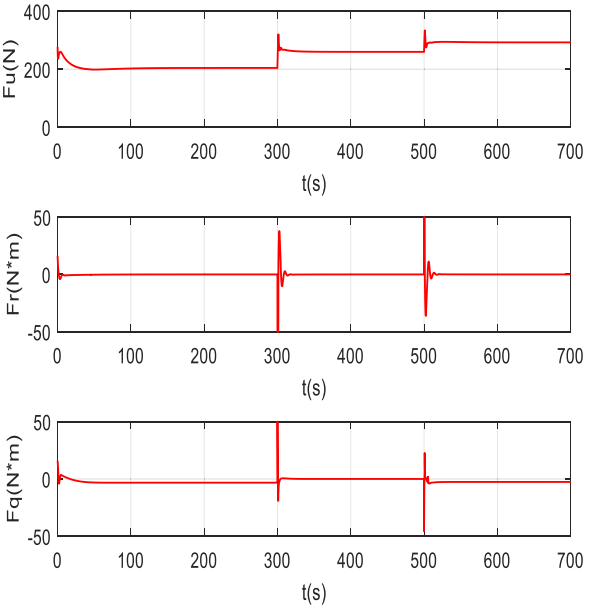

FIGURE 16. Force and torque input.

Fig. 18 is the trajectory of UUV tracking space curve. The blue dotted line is the desired trajectory, and the red solid line is the actual trajectory of UUV.

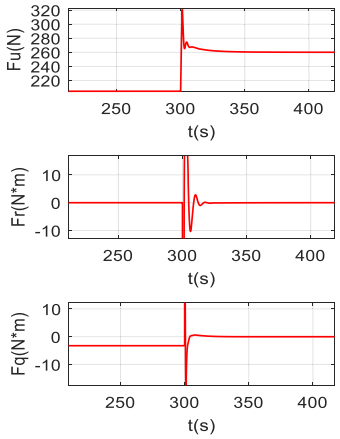

FIGURE 17. Partial enlarged version of fig.16.

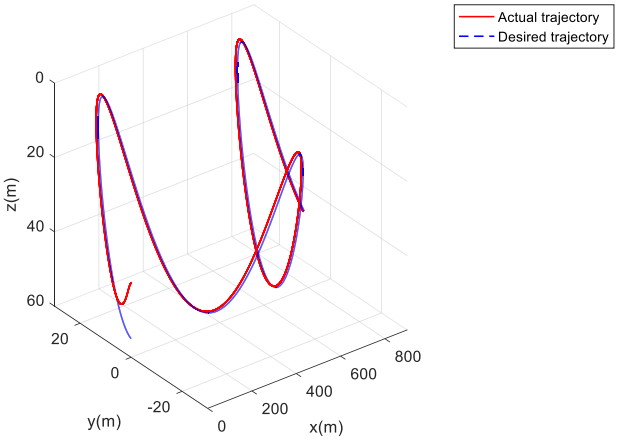

FIGURE 18. UUV trajectory.

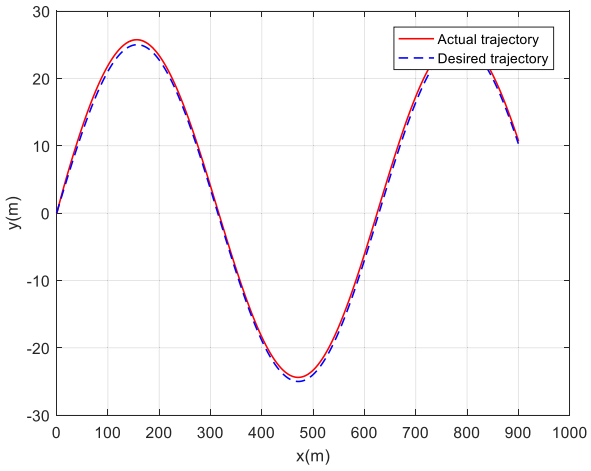

FIGURE 19. Motion trajectory projection on xoy axis.

Fig. 19 and Fig. 20 are projections of UUV tracking trajectories on horizontal and vertical planes respectively. At the initial time, the position error between UUV and desired trajectories is large, then the desired trajectory position error begins to move and coincide with desired trajectories quickly. It shows that UUV can track spatial curves more quickly under current disturbance.

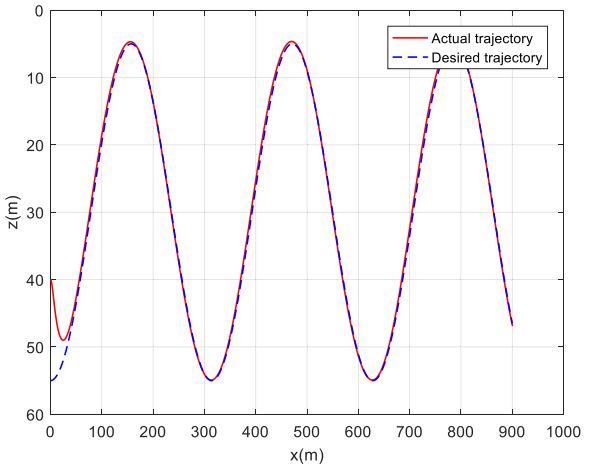

FIGURE 20. Motion trajectory projection on xoy axis.

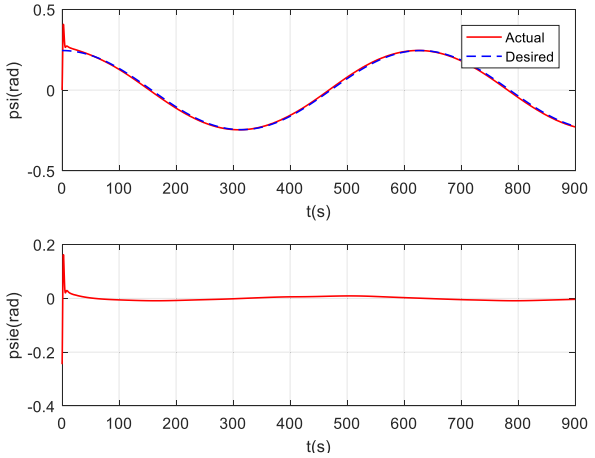

FIGURE 21. Yaw angle and angle error.

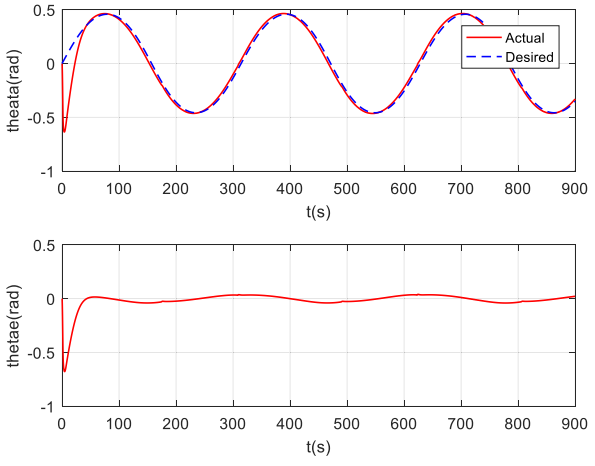

FIGURE 22. Pitch angle and angle error.

Fig. 21 and Fig. 22 are UUV yaw angle, pitch angle and their error response curves respectively. Under steady current disturbance, heading control can be achieved without sustained rapid oscillation of yaw angle. However, due to the disturbance of steady current, the transverse velocity of UUV increases, so the drift angle component becomes larger. In the

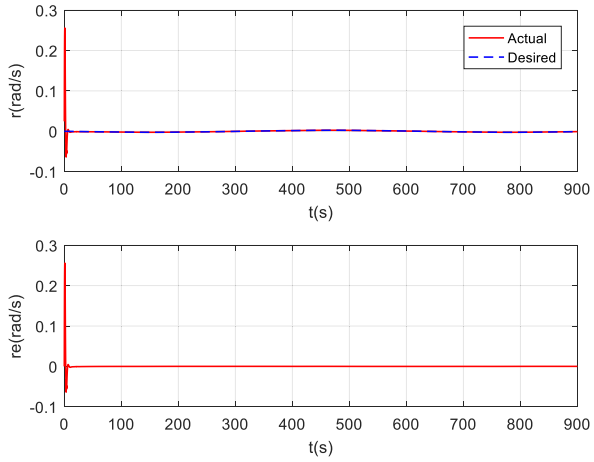

FIGURE 23. Yaw angular velocity and velocity error.

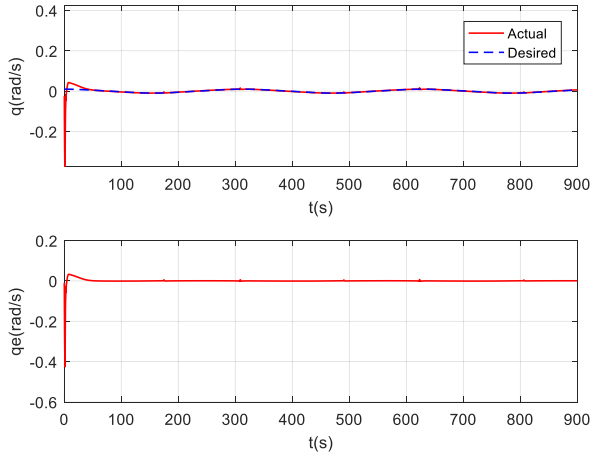

FIGURE 24. Pitch angular velocity and velocity error.

design of three-dimensional guidance method, drift angle is neglected in order to simplify the calculation. The difference increased slightly.

Fig. 23 and Fig. 24 are UUV yaw angle, pitch angle velocities and their error response curves respectively. In the initial stage, the angular velocity varies most dramatically, because the attitude of the initial UUV differs greatly from the desired attitude, and is affected by the initial position and velocity errors. The angular velocity varies sharply, but the steady-state error of the angular velocity does not exceed 0.02.

Fig. 25 shows the response curve of UUV tracking position error. It can be seen that there are some errors in the three axes in the fixed coordinate system. The east-direction position error is obviously larger than the north-direction error, which is related to the underactuation of UUV.

Fig. 26, 27 and 28 are the response curves of UUV longitudinal, transverse, vertical velocity and velocity errors respectively. It can be seen that the transverse velocity errors are obvious. When UUV moves in a curve, it will inevitably produce drift angle components. At this time, the transverse velocity is no longer zero, and the vertical motion is similar to the transverse motion. Because the vertical motion is linear, the impact angle is zero.

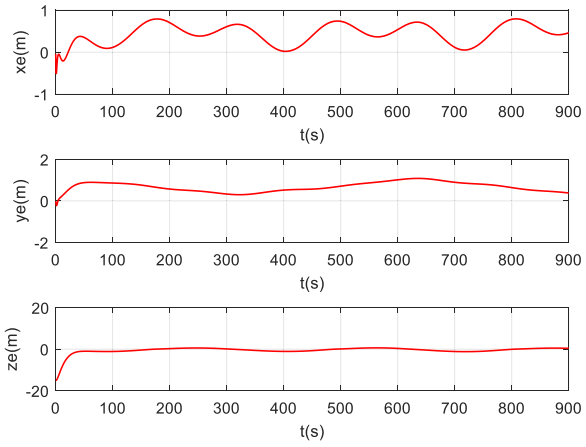

FIGURE 25. UUV position error.

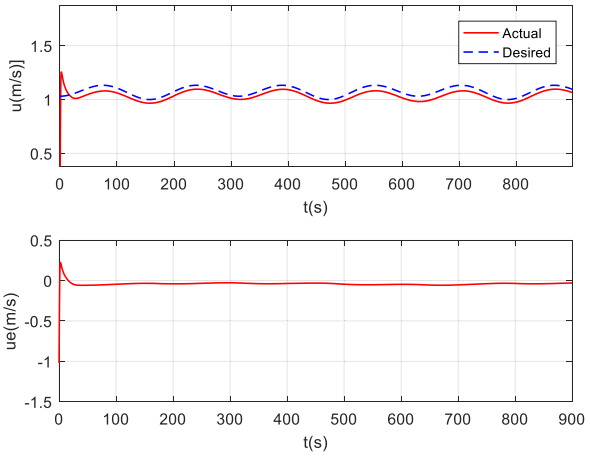

FIGURE 26. Surge velocity and velocity error.

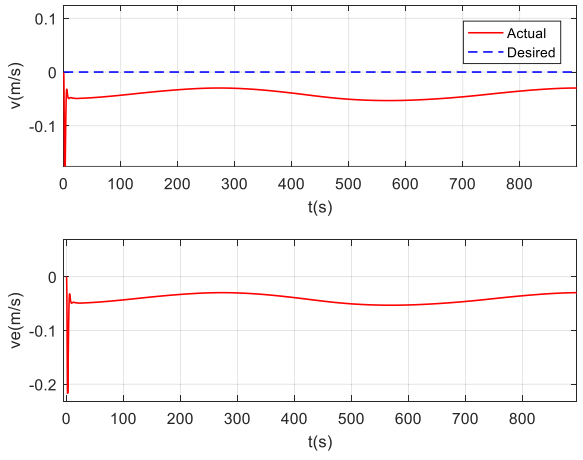

FIGURE 27. Surge velocity and velocity error.

Fig. 29 and Fig. 30 are UUV control force and moment input curves respectively. In the initial stage, the curve changes a lot, because UUV starts moving from the static state and needs to reach the desired state quickly. In the steady-state stage, the control force and moment change smoothly. Because the tangential velocity of the tracking curve changes obviously, the corresponding control moment

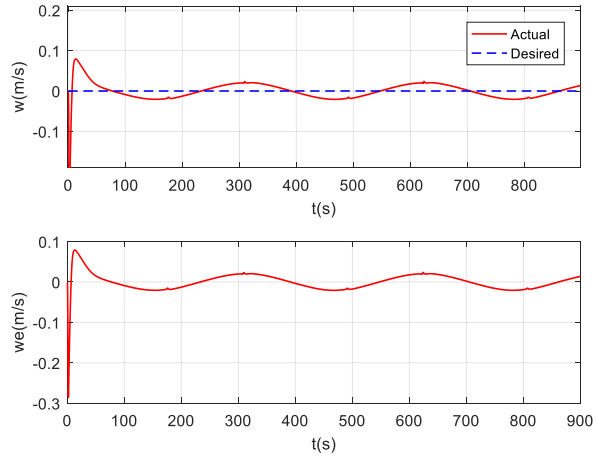

FIGURE 28. Heave velocity and velocity error.

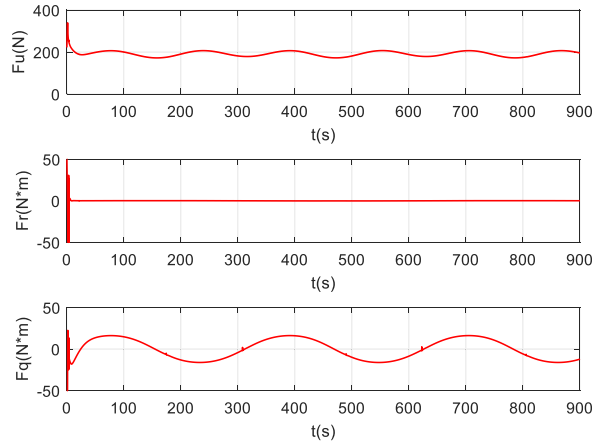

FIGURE 29. Force and torque input.

fluctuates greatly, and the control curve almost has no chattering in the whole process.

In a word, it can be found integral sliding mode control method is better than backstepping control method by comparing the simulation results. What's more, it is simple to design the integral sliding mode controller.

V. CONCLUSION

In this paper, a backstepping sliding mode controller with double-loop structure is designed to solve the problem of under-actuation and external current disturbance in UUV trajectory tracking control. The outer-loop position constructs Lyapunov function position error based on space position error in fixed coordinate system, and obtains virtual control law. The inner-loop velocity constructs linear velocity integral sliding surface stabilization velocity error by tracking virtual control law. Finally, the effectiveness of the control method is verified by analyzing the simulation experiment of space trajectory tracking. Used the integral sliding mode surface to guarantee the asymptotic convergence of the tracking errors in this paper. The next stage of our research is to ensure the finite-time convergence of tracking errors.

REFERENCES

[1] A. P. Aguiar and J. P. Hespanha, "Trajectory-tracking and path-following of underactuated autonomous vehicles with parametric modeling uncertainty," *IEEE Trans. Autom. Control*, vol. 52, no. 8, pp. 1362–1379, Aug. 2007.
[2] F. Repoulias and E. Papadopoulos, "Planar trajectory planning and tracking control design for underactuated AUVs," *Ocean Eng.*, vol. 34, nos. 11–12, pp. 1650–1667, Aug. 2007.
[3] X. Jian, W. Man, and Q. Lei, "Three-dimensional trajectory tracking of an underactuated UUV by backstepping control," *Control Theory Appl.*, vol. 31, no. 11, pp. 1589–1596, 2014.
[4] F. Repoulias and E. Papadopoulos, "Three dimensional trajectory control of underactuated AUVs," in *Proc. IEEE Eur. Control Conf.*, Kos, Greece, Jul. 2007, pp. 3492–3499.
[5] J. Zhou, D. Ye, D. He, and D. Xu, "Three-dimensional trajectory tracking of an underactuated UUV by backstepping control and bio-inspired models," in *Proc. China Control Conf.*, Jul. 2017, pp. 966–972.
[6] W. Zhang, T. Yanbin, W. Shilin, S. Hu, and J. Zhang, "Underactuated UUV tracking control of adaptive RBF neural network and backstepping method," *J. Harbin Eng. Univ.*, vol. 39, no. 1, pp. 93–99, Jan. 2018.
[7] H.-M. Jia, W.-L. Song, and J.-J. Zhou, "Bottom following control for an underactuated AUV based on nonlinear backstepping method," *J. Beijing Univ. Technol.*, vol. 38, no. 12, pp. 1708–1785, 2012.
[8] R. Wang, S. Wang, Y. Wang, M. Tan, and J. Yu, "A paradigm for path following control of a ribbon-fin propelled biomimetic underwater vehicle," *IEEE Trans. Syst., Man, Cybern. Syst.*, vol. 49, no. 3, pp. 482–493, Mar. 2019.
[9] H. Ashrafiuon, K. R. Muske, L. C. McNinch, and R. A. Soltan, "Sliding-mode tracking control of surface vessels," *IEEE Trans. Ind. Electron.*, vol. 55, no. 11, pp. 4004–4012, Nov. 2008.
[10] J. Xu, M. Wang, and L. Qiao, "Dynamical sliding mode control for the trajectory tracking of underactuated unmanned underwater vehicles," *Ocean Eng.*, vol. 105, pp. 54–63, Sep. 2015.
[11] L. Qiao and W. Zhang, "Double-loop chattering-free adaptive integral sliding mode control for underwater vehicles," in *Proc. IEEE Oceans*, Shanghai, China, Apr. 2016, pp. 1–6.
[12] T. Elmokadem, M. Zribi, and K. Youcef-Toumi, "Terminal sliding mode control for the trajectory tracking of underactuated autonomous underwater vehicles," *Ocean Eng.*, vol. 129, pp. 613–625, Jan. 2017.
[13] M. Kim, H. Joe, J. Kim, and S.-C. Yu, "Integral sliding mode controller for precise manoeuvring of autonomous underwater vehicle in the presence of unknown environmental disturbances," *Int. J. Control*, vol. 88, no. 10, pp. 2055–2065, 2015.
[14] M. R. Ramezani-Al and Z. T. Sereshki, "A novel adaptive sliding mode controller design for tracking problem of an AUV in the horizontal plane," *Int. J. Dyn. Control*, vol. 7, no. 2, pp. 679–689, 2019.
[15] Y. Zhe-Ping and D. Hai-Pu, "Double-loop terminal sliding mode control for the trajectory tracking of UUV," *Chin. Ship Res.*, vol. 4, pp. 112–117, 2015.
[16] M. N. Nounou, H. Nounou, and M. S. Mahmoud, "Robust adaptive sliding-mode control for continuous time-delay systems," *IMA J. Math. Control Inf.*, vol. 24, no. 3, pp. 299–313, 2018.
[17] J. Fei and C. Lu, "Adaptive sliding mode control of dynamic systems using double loop recurrent neural network structure," *IEEE Trans. Neural Netw. Learn. Syst.*, vol. 29, no. 4, pp. 1275–1286, Apr. 2018.
[18] K. Y. Pettersen and O. Egeland, "Time-varying exponential stabilization of the position and attitude of an underactuated autonomous underwater vehicle," *IEEE Trans. Autom. Control*, vol. 44, no. 1, pp. 112–115, Jan. 1999.
[19] L. Qiao and W. Zhang, "Adaptive second-order fast nonsingular terminal sliding mode tracking control for fully actuated autonomous underwater vehicles," *IEEE J. Ocean. Eng.*, vol. 44, no. 2, pp. 363–385, Apr. 2019.
[20] L. Qiao and W. Zhang, "Double-loop integral terminal sliding mode tracking control for UUVs with adaptive dynamic compensation of uncertainties and disturbances," *IEEE J. Ocean. Eng.*, vol. 44, no. 1, pp. 29–53, Jan. 2019.
[21] L. Qiao and W. Zhang, "Adaptive non-singular integral terminal sliding mode tracking control for autonomous underwater vehicles," *IET Control Theory Appl.*, vol. 11, no. 8, pp. 1293–1306, Feb. 2017.